SIAM J. APPL. MATH.
Vol. 66, No. 1, pp. 57–81

WEAKLY INTERACTING PULSES IN SYNAPTICALLY COUPLED NEURAL MEDIA*

PAUL C. BRESSLOFF†

Abstract. We use singular perturbation theory to analyze the dynamics of N weakly interacting pulses in a one-dimensional synaptically coupled neuronal network. The network is modeled in terms of a nonlocal integro-differential equation, in which the integral kernel represents the spatial distribution of synaptic weights, and the output activity of a neuron is taken to be a mean firing rate. We derive a set of N coupled ordinary differential equations (ODEs) for the dynamics of individual pulses, establishing a direct relationship between the explicit form of the pulse interactions and the structure of the long-range synaptic coupling. The system of ODEs is used to explore the existence and stability of stationary N-pulses and traveling wave trains.

Key words. neural networks, localized spiral patterns, traveling pulses, integro-differential equations

AMS subject classification. 92C20

DOI. 10.1137/040616371

1. Introduction.

Synaptically coupled neuronal networks provide an important example of spatially extended excitable systems with nonlocal interactions. The network dynamics is usually modeled in terms of an integro-differential equation, in which the integral kernel represents the spatial distribution of synaptic weights and the output activity of a neuron is taken to be a mean firing rate [41, 12]. As in the case of nonlinear PDE models of diffusively coupled excitable systems [23], neuronal networks can exhibit a variety of coherent pulse-like structures including both stationary and traveling solitary pulses. Traveling pulses tend to occur when synaptic connections are predominantly excitatory and there is some form of slow local adaptation or recovery [34, 7], whereas stationary pulses occur in the presence of lateral inhibition [1, 35, 40]. Analogous solutions are found in integrate-and-fire networks, where the output of a neuron is taken to be a sequence of spikes rather than a firing rate [13, 4, 24]. The formation of localized activity states can be used to model a number of neurobiological phenomena. For example, traveling pulses have been observed in disinhibited slice preparations [6, 20, 42] using voltage-sensitive dyes and multiple electrodes. An individual pulse is generated by a brief current stimulus, whereas a train of pulses occurs in the case of repeated stimulation. A second example is given by a delayed response task, in which an animal is required to retain information about a sensory cue across a delay period between the stimulus and behavioral response. Physiological recordings in prefrontal cortex have shown that spatially localized groups of neurons fire during the recall task and then stop firing once the task has finished [18, 39]. Thus persistent localized states of activity are thought to be neural correlates of spatial working memory. An interesting question then concerns the nature of the interactions between multiple regions of localized activity induced by more complex stimuli.

Although there are an increasing number of studies regarding the behavior of solitary pulses in excitable neural media, there is relatively little known about multipulse

*Received by the editors October 5, 2004; accepted for publication (in revised form) April 13, 2005; published electronically October 3, 2005.
http://www.siam.org/journals/siap/66-1/61637.html
†Department of Mathematics, University of Utah, 155 S. 1400 E, Salt Lake City, UT 84112 (bressloff@math.utah.edu).

solutions. One approach to studying stationary N-pulse solutions in rate models is to convert the integro-differential equation into a corresponding fourth-order PDE by an appropriate choice of weight distribution, and then to search for global homoclinic connections [25, 26, 7] or bifurcations from single-pulse solutions [27]. This approach has established, for example, that stable N-pulse solutions can occur when lateral inhibition is modulated by a spatially oscillating component.

In this paper we analyze multipulse solutions of a one-dimensional neuronal network with a Heaviside firing rate function, under the assumption that the individual pulses are well separated so that their mutual interactions are weak. We use singular perturbation theory to derive equations of motion for the pulse positions, in order to investigate the existence and stability of stationary and traveling N-pulse solutions. Our analysis provides a nontrivial extension of previous studies of weakly interacting pulses in nonlinear PDE models of diffusively coupled excitable media and fluids [9, 10, 2, 3, 37, 33]. First, it applies to a nonlocal integro-differential equation that cannot be reduced to a finite-order PDE except for very specific choices of the synaptic weight distribution. Second, using a Heaviside firing rate function, it is possible to obtain exact solutions for single-pulse profiles and to carry out explicit calculations in the derivation of the dynamical equations for weakly interacting pulses. Third, and most significantly from a biological perspective, there is a direct relationship between the nature of the pulse interactions and the form of the long-range synaptic coupling.

We focus in this paper on three distinct but related models that correspond to three distinct experimental paradigms. In section 2, we analyze stationary pulses in a network with symmetric lateral inhibition, which can be interpreted as a simple model of persistent working memory. Assuming that the weights decay exponentially at large distances, the corresponding single-pulse profile also decays exponentially so that widely separated pulses interact weakly. Using singular perturbation theory, we show how the existence and stability of stationary N-pulses reduces to the problem of finding fixed points of a set of N coupled ODEs describing the motion of individual pulses. This is considerably simpler than looking for multipulse solutions of the full nonlocal equation [25, 26, 7]. Consistent with these other studies, we find that in the presence of pure lateral inhibition well separated pulses repel each other, so that a stable N-pulse solution cannot exist. On the other hand, in the case of a spatially decaying oscillatory weight distribution, stable N-pulses can occur. In section 3, we extend our analysis to the case of a network with asymmetric lateral inhibition, which has been proposed as a model of direction selective neurons in visual cortex [38, 30, 32, 43]. Localized activity pulses now tend to propagate unidirectionally rather than remain stationary. Extending the analysis of section 2 by working in the moving frame of a single traveling pulse, we derive the corresponding system of ODEs for N weakly interacting traveling pulses. These equations are then used to explore the existence and stability of traveling wave trains, with the separation between successive pulses characterized by a lattice map [10]. In the case of spatially oscillatory weights, such a map could potentially exhibit both regular and chaotic behavior. In section 4, we consider an excitatory network with an additional adaptation variable, which has been used to model wave propagation in disinhibited cortical slices [34]. In contrast to the asymmetric lateral inhibition network, waves can now travel in both directions. The resulting system of ODEs for N interacting pulses is identical in form to the previous case, but the asymptotic behavior of a single pulse profile is different. In particular, the leading edge of the pulse decays much more rapidly than the trailing edge, which also typically holds for traveling pulses in diffusively coupled excitable systems [23]. This difference in decay rates can be used to reduce the dynamics to a

kinematic form [11, 33].

2. Stationary pulses in symmetric lateral inhibition networks. Let $u(x,t)$ represent the local activity of a population of neurons at position $x \in \mathbf{R}$ in a one-dimensional neuronal network. Suppose that u evolves according to the integro-differential equation

$$\tau_m \frac{\partial u(x,t)}{\partial t} = -u(x,t) + \int_{-\infty}^{\infty} w(x-x')H[u(x',t)-\kappa]dx', \tag{2.1}$$

where τ_m is a membrane or synaptic time constant, κ is a threshold, $H(u)$ denotes the output firing rate, and $w(x-x')$ is the strength of connections from neurons at x' to neurons at x. We assume that w is a continuous function satisfying $w(-x) = w(x)$ and $\int_{-\infty}^{\infty} w(x) < \infty$. The nonlinearity H is taken to be the Heaviside function

$$H[u] = \begin{cases} 0 & \text{if } u \le 0, \\ 1 & \text{if } u > 0. \end{cases} \tag{2.2}$$

In the following we treat length and time in dimensionless units. First, we set $\tau_m = 1$ so that the unit of time is of the order 10msec. Second, the range of the synaptic coupling introduces a fundamental length scale, which we use to set the unit of length to be of the order 200μm.

Equation (2.1) was first analyzed in detail by Amari [1], who showed that there exist stationary solitary pulse solutions when the weight distribution $w(x)$ is given by a Mexican hat function:

(i) $w(x) > 0$ for $x \in [0, x_0)$ with $w(x_0) = 0$,
(ii) $w(x) < 0$ for $x \in (x_0, \infty)$,
(iii) $w(x)$ is decreasing on $[0, x_0]$,
(iv) $w(x)$ has a unique minimum on $\mathbf{R}^+$ at $x = x_1$ with $x_1 > x_0$ and $w(x)$ strictly increasing on (x_1, ∞).

More recently, it has been established that (2.1) can also support stable stationary N-pulse solutions, provided that the weight distribution has additional zeros, which would occur if there were an oscillatory modulation of the long-range connections [25, 26, 27]. We will refer to any network that has long-range inhibition (possibly alternating with long-range excitation) as a lateral inhibition network. In this section we use singular perturbation theory to analyze the dynamics of N-pulse solutions of (2.1), under the assumption that the interactions between pulses are weak. We show that in the case of a Mexican hat weight distribution, the pulses mutually repel each other so that stable N-pulse solutions cannot occur. On the other hand, when the weight distribution consists of decaying spatial oscillations, there exist configurations of the pulse locations (up to a global translation) corresponding to stable N-pulse bound states. This result is consistent with the findings of Laing et al. [25] and Laing and Tray [26, 27].

2.1. Stationary solitary pulses. Suppose that $U(x)$ is a stationary solution of (2.1): $u(x,t) = U(x)$ with

$$U(x) = \int_{-\infty}^{\infty} w(x-x')H[U(x')-\kappa]dx'. \tag{2.3}$$

Let $\mathcal{M}[U] = \{x | U(x) > \kappa\}$ be the region over which the activity U is excited (superthreshold). Equation (2.3) can then be rewritten as

$$U(x) = \int_{\mathcal{M}[U]} w(x-x')dx'. \tag{2.4}$$

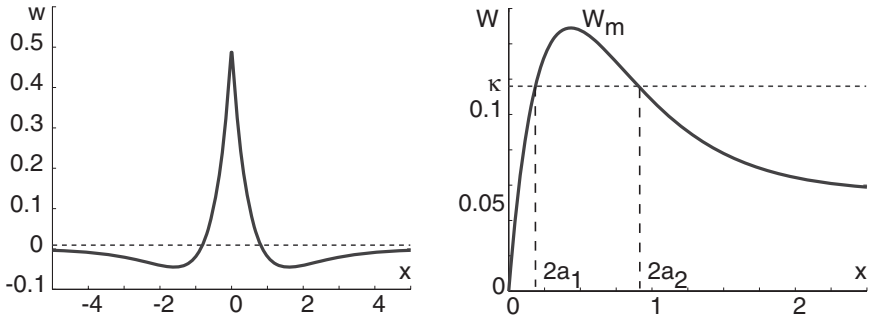

FIG. 2.1. *Construction of stationary pulses for a Mexican hat weight distribution.* (a) *Plot of* $w(x)$ *given by the difference-of-exponentials* (2.8) *with* $\sigma_E = 1.8, \sigma_I = 1.0$, *and* $\Gamma = 0.5$. (b) *Plot of corresponding function* $W(x)$. *Horizontal line shows the threshold* κ *whose intersections with* $W(2a)$ *determine the allowed pulse widths.*

We define a single pulse solution of width $2a$ to be one that is excited over the interval $(-a, a)$; any pulse solution can be arbitrarily translated so that it is centered at the origin. If we set

$$W(x) = \int_0^x w(y)dy, \tag{2.5}$$

then (2.4) reduces to the form

$$U(x) = W(a + x) - W(x - a). \tag{2.6}$$

Note that $W(0) = 0$ and $W(-x) = -W(x)$. Since $U(\pm a) = \kappa$, we obtain the following necessary condition for the existence of a stationary pulse of width $2a$:

$$W(2a) = \kappa. \tag{2.7}$$

Amari [1] showed that in the case of a Mexican hat weight distribution this condition is also sufficient. He also established that a stationary pulse is stable, provided that $W'(a) \equiv w(a) < 0$; otherwise it is unstable.

The stable and unstable pulses can be determined graphically, as illustrated in Figure 2.1 for a Mexican hat function w given by the difference-of-exponentials

$$w(x) = \mathrm{e}^{-\sigma_E|x|} - \Gamma \mathrm{e}^{-\sigma_I|x|}, \tag{2.8}$$

with $\sigma_E > \sigma_I > 0$ and $0 < \Gamma < 1$. Here σ_E^{-1} and σ_I^{-1} determine the range of excitatory and inhibitory synaptic coupling, respectively. If one neglects long-range horizontal connections (see below), then such coupling tends to extend up to around 0.8mm in cortex [29]. Integrating (2.8), we have

$$W(x) = \frac{1}{\sigma_E}\left[1 - \mathrm{e}^{-\sigma_E x}\right] - \frac{\Gamma}{\sigma_I}\left[1 - \mathrm{e}^{-\sigma_I x}\right] \tag{2.9}$$

for $x \geq 0$. The existence of single-pulse solutions depends on the relative sizes of W_m, W_∞, and κ, where

$$W_m = \max_{x>0} W(x), \quad W_\infty = \lim_{x\to\infty} W(x) = \frac{1}{\sigma_E} - \frac{\Gamma}{\sigma_I}. \tag{2.10}$$

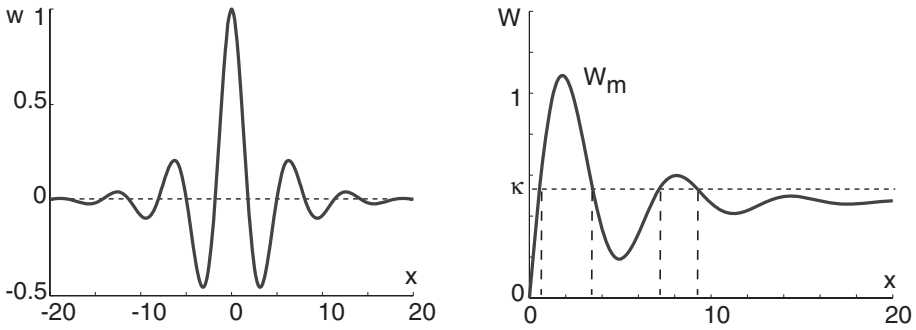

FIG. 2.2. *Construction of a stationary pulse for a spatially decaying oscillatory weight distribution.* (a) *Plot of* $w(x)$ *given by* (2.11) *with* $\sigma = 0.25$. (b) *Plot of corresponding function* $W(x)$. *The horizontal line shows the threshold* κ *whose intersections with* $W(2a)$ *determine the allowed pulse widths.*

If $0 < W_\infty < \kappa < W_m$, then there exists an unstable pulse of width a_1 and a stable pulse of width a_2 with $a_2 > a_1$, whereas there is only an unstable pulse when $0 < \kappa < W_\infty$. In the latter case the network is in a bistable regime, where the unstable pulse acts as a separatrix between a stable uniform resting state ($U \equiv 0$) and a traveling front. If $W_\infty < \kappa < 0 < W_m$, then there is a stable pulse but no unstable pulse. Outside these parameter regimes there are no pulses.

In Figure 2.2, we illustrate the corresponding graphical construction for a spatially decaying oscillatory weight distribution of the form [25]

$$w(x) = \mathrm{e}^{-\sigma|x|}\left[\cos(x) + \sigma \sin|x|\right]. \tag{2.11}$$

Integrating (2.11), we have

$$W(x) = \frac{2\sigma}{1+\sigma^2}\left[1 - \mathrm{e}^{-\sigma x}\cos(x)\right] + \frac{1-\sigma^2}{1+\sigma^2}\mathrm{e}^{-\sigma x}\sin(x), \quad x \geq 0, \tag{2.12}$$

with $W(-x) = -W(x)$. It can be seen from Figure 2.2 that, as κ is reduced below W_m, an increasing number of stable/unstable pairs of pulses are generated, assuming that condition (2.7) is sufficient to ensure $U(x) > \kappa$ for $|x| < a$ and $U(x) < \kappa$ for $|x| > a$. This has not been proven analytically for the weight distribution (2.11), although the existence of stable pulses has been confirmed numerically by Laing et al. [25]. These authors have also suggested that an anatomical substrate for the oscillatory weight distribution (2.11) might be the long-range horizontal connections found in superficial layers of cortex. Such connections extend several millimeters across cortex and are broken into discrete patches with a very regular size and spacing [36, 19, 28]. Although the horizontal connections arise almost exclusively from excitatory neurons, 20% of them terminate on interneurons that can generate significant inhibition [31]. Whether the horizontal connections have a net inhibitory or excitatory effect does not appear to be a simple function of cortical separation, however, since it also depends on the local level of activity of neurons innervated by the long-range connections [29]. Therefore, certain care has to be taken in the biological interpretation of the weight distribution (2.11).

2.2. Singular perturbation theory. Suppose that (2.1) has a stable stationary pulse solution $U(x)$ of width $2a$ centered at the origin such that in the large-$|x|$ limit,

the activity of the pulse decays exponentially, $|U(x)| \sim \mathrm{e}^{-\rho|x|}$. For example, $\rho = \sigma_I$ in the case of the Mexican hat function (2.8), and $\rho = \sigma$ in the case of the spatially decaying oscillatory function (2.11). This suggests that if two or more such pulses are placed on the real line such that the characteristic separation d between the centers of any two pulses satisfies $\mathrm{e}^{-\rho d} = \varepsilon \ll 1$, then the interactions between the pulses will be weak. In the weakly interacting regime, we can carry out a perturbation analysis of the dynamics along lines analogous to those used by Elphick, Meron, and Spiegel [10] by treating ε as a small parameter.

Following [10], we look for an N-pulse solution with individual pulses having centers at $x_n = nd + \phi_n(\tau)$, where $\phi_n(\tau)$ is a slowly varying phase and $\tau = \varepsilon t$. That is, we consider a train of pulses

$$u(x,\tau) = \sum_{n=1}^{N} U(x - nd - \phi_n(\tau)) + \varepsilon R(x,\tau). \tag{2.13}$$

The remainder term εR takes into account the fact that a superposition of widely separated pulses cannot be an exact solution, even when we allow for slowly drifting phases ϕ_n. Substituting (2.13) into (2.1) with $\partial_t \to \partial_t + \varepsilon\partial_\tau$, and using (2.3), gives

$$\varepsilon^2\partial_\tau R - \varepsilon\sum_{n=1}^{N}\dot{\phi}_n U_n' = -\varepsilon R + w * H\left(\sum_{n=1}^{N} U_n + \varepsilon R - \kappa\right) - w * \sum_{n=1}^{N} H(U_n - \kappa), \tag{2.14}$$

where $U_n(x) = U(x - nd - \phi_n(\tau))$ and $w * g$ denotes the convolution

$$w * g = \int_{-\infty}^{\infty} w(x - x')g(x')dx'. \tag{2.15}$$

We now carry out a perturbation expansion in ε by formally Taylor expanding with respect to εR inside the convolution integral:

$$w * H\left(\sum_{n=1}^{N} U_n - \kappa + \varepsilon R\right) = w * \left[H\left(\sum_{n=1}^{N} U_n - \kappa\right) + \varepsilon\delta\left(\sum_{n=1}^{N} U_n - \kappa\right) R + \mathcal{O}\left(\varepsilon^2\right)\right], \tag{2.16}$$

where δ is the Dirac delta function. This formal series expansion can be interpreted along the following lines. First, we assume that in the case of widely separated pulses, the multibump function $V \equiv \sum_n U_n(x)$ has N pairs of threshold crossing points $x_m^{\pm} \approx x_m \pm a$ such that $V(x) > \kappa$ for $x_m^- < x < x_m^+$, $V(x_m^{\pm}) = \kappa$ and $V(x) < \kappa$ otherwise. It follows that

$$\delta(V(x) - \kappa) = \sum_{m=1}^{N}\left[\frac{\delta(x - x_m^+)}{|V'(x_m^+)|} + \frac{\delta(x - x_m^-)}{|V'(x_m^-)|}\right]. \tag{2.17}$$

Similarly, the function $V + \varepsilon R$ is assumed to have threshold crossing points at $x_m^{\pm} + \varepsilon\Delta_m^{\pm}$. The convolution integral then has the explicit form

$$\begin{aligned} w * H\left(\sum_{n=1}^{N} U_n - \kappa + \varepsilon R\right)(x) &= \sum_{n=1}^{N}\int_{x_n^- + \varepsilon\Delta_n^-}^{x_n^+ + \varepsilon\Delta_n^+} w(x - x')dx' \\ &= \sum_{n=1}^{N}\int_{x_n^-}^{x_n^+} w(x - x')dx' \\ &\quad + \varepsilon\left[w(x - x_n^+)\Delta_n^+ - w(x - x_n^-)\Delta_n^-\right] + \mathcal{O}(\varepsilon^2), \end{aligned} \tag{2.18}$$

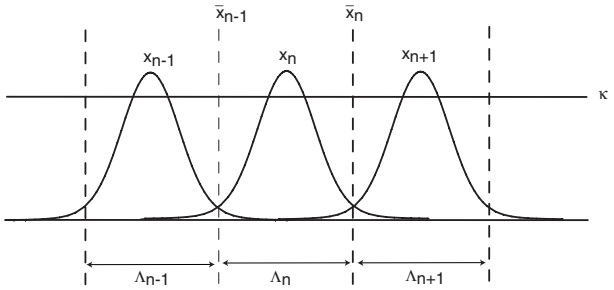

FIG. 2.3. *Illustrative sketch of a multibump solution in which the nth activity bump (region above threshold κ) is localized within the domain Λ_n. In a neighborhood of the mth activity bump we assume that $U_n(x) \sim \varepsilon^{|m-n|}$ for $m \neq n$, where $U_n(x) = U(x - x_n)$ and x_n is the center of the nth bump.*

where we have Taylor expanded with respect to the perturbations $\varepsilon\Delta_m^{\pm}$ in the locations of the activity bump boundaries. Substituting (2.17) into (2.16) shows that the latter is equivalent to (2.18) with $\Delta_m^+ = R(x_m^+)/|V'(x_m^+)|$ and $\Delta_m^- = -R(x_m^-)/|V'(x_m^-)|$.

Substituting (2.16) into (2.14) and collecting first-order terms in ε leads to the following inhomogeneous equation for R:

$$\widehat{L}R = \sum_{n=1}^{N} \dot{\phi}_n U_n' + \frac{1}{\varepsilon} w * \left[H\left(\sum_{n=1}^{N} U_n - \kappa \right) - \sum_{n=1}^{N} H(U_n - \kappa) \right], \tag{2.19}$$

where $\widehat{L}$ is the linear operator

$$\widehat{L}\psi = \psi - w * \left(\delta\left(\sum_{n=1}^{N} U_n - \kappa \right) \psi \right) \tag{2.20}$$

for any function $\psi \in L^2(\mathbf{R})$. We now show that the term in square brackets on the right-hand side of (2.19) is $\mathcal{O}(\varepsilon)$. First, partition the real line into nonoverlapping domains such that the mth activity bump lies entirely in the domain Λ_m, as illustrated in Figure 2.3. More specifically, take $\mathbf{R} = \cup_{m=1}^{N} \Lambda_m$ with $\Lambda_m = [\bar{x}_{m-1}, \bar{x}_m)$ for $m = 2, \ldots, N-1$, $\Lambda_1 = (-\infty, \bar{x}_1)$, and $\Lambda_N = (\bar{x}_{N-1}, \infty)$. Here $\bar{x}_m = (x_{m+1} - x_m)/2$ is the midpoint between neighboring bumps. The characteristic pulse separation d is assumed to be sufficiently large such that $U_n(x) \sim \varepsilon^{|m-n|}$ in a neighborhood of the mth activity bump for $m \neq n$. The given partition then allows us to carry out a formal perturbation expansion along lines similar to (2.16):

$$\begin{aligned}
&\int_{-\infty}^{\infty} w(x - x') H\left(\sum_n U_n(x') - \kappa \right) dx' = \sum_{m=-\infty}^{\infty} \int_{\Lambda_m} w(x - x') H\left(\sum_n U_n(x') - \kappa \right) dx' \\
&= \sum_{m=-\infty}^{\infty} \int_{\Lambda_m} w(x - x') H\left(U_m(x') + \sum_{n \neq m} U_n(x') - \kappa \right) dx' \\
&= \sum_{m=-\infty}^{\infty} \int_{\Lambda_m} w(x - x') \left(H(U_m(x') - \kappa) + \delta(U_m(x') - \kappa) \sum_{n=m\pm1} U_n(x') + \mathcal{O}(\varepsilon^2) \right) dx'.
\end{aligned} \tag{2.21}$$

Only nearest neighbor bumps contribute to the $\mathcal{O}(\varepsilon)$ term. The delta function $\delta(U_m(x)-\kappa)$ can be simplified using the threshold condition $U_m(\pm a+x_m)=\kappa$:

$$\delta(U_m(x)-\kappa)=\frac{\delta(x-a-x_m)}{|U'(a)|}+\frac{\delta(x+a-x_m)}{|U'(-a)|}. \tag{2.22}$$

Since $U_m(x)<\kappa$ for all $x\notin\Lambda_m$, we can replace the integral domain Λ_m in each of the integrals in (2.21) by the whole real line $(-\infty,\infty)$. Thus we find

$$w*H\left(\sum_{n=1}^{N}U_n-\kappa\right)=w*\left[\sum_{n=1}^{N}H(U_n-\kappa)+\sum_{n=1}^{N}\delta(U_n-\kappa)[U_{n+1}+U_{n-1}]+\mathcal{O}(\varepsilon^2)\right] \tag{2.23}$$

with $U_{N+1},U_0\equiv 0$.

In order for the above perturbation expansion to be valid, we require that the correction term R be finite everywhere. Following Elphick, Meran, and Spiegel [10], we will show how this implies a set of solvability conditions on (2.19), which in turn determine the leading-order dynamics of the phases ϕ_n or, equivalently, the pulse positions x_n. In order to gain insights into the analytical properties of the linear operator $\widehat{L}$ it is useful to consider the simpler operator $\widehat{L}_n$, where

$$\widehat{L}_n\psi=\psi-w*[\delta(U_n-\kappa)\psi]. \tag{2.24}$$

The latter has zero as an eigenvalue with corresponding eigenfunction $Q=U_n'$, which can be seen by differentiating (2.3). Therefore, the eigenvalue equation $\widehat{L}Q=\lambda Q$ has approximate solutions of the form $Q=\sum_{i=1}^{N}c_nU_n'$, where c_n are constants, with associated eigenvalues $\lambda=\mathcal{O}(\varepsilon)$. Assuming the standard inner product of functions P,Q on $\mathbf{R}$,

$$\langle P|Q\rangle=\int_{-\infty}^{\infty}P(x)Q(x)dx, \tag{2.25}$$

we define the adjoint operator $\widehat{L}^\dagger$ according to

$$\langle P|\widehat{L}Q\rangle=\langle\widehat{L}^\dagger P|Q\rangle, \tag{2.26}$$

so that

$$\widehat{L}^\dagger\psi=\psi-\delta\left(\sum_{n=1}^{N}U_n-\kappa\right)w*\psi. \tag{2.27}$$

The existence of N null vectors of $\widehat{L}_n$ suggests that its adjoint should also have N null vectors, which can then be used to construct eigenfunctions of $\widehat{L}^\dagger$ with $\mathcal{O}(\varepsilon)$ eigenvalues. However, since the operator $\widehat{L}_n$ is not self-adjoint, one cannot assume a priori that it has index zero. The situation is further complicated by the fact that $\widehat{L}^\dagger$ involves distributions. Therefore, we will proceed by searching for weak solutions P of the equation

$$\langle\widehat{L}^\dagger P|Q\rangle=\mathcal{O}(\varepsilon) \tag{2.28}$$

for any bounded function Q.

Comparison of (2.17) and (2.22) shows that in the weakly interacting regime,

$$\int \psi(x)\delta\left(\sum_n U_n(x)-\kappa\right)dx = \int \psi(x)\sum_{n=1}^{N}\delta\left(U_n(x)-\kappa\right)dx+\mathcal{O}(\varepsilon) \tag{2.29}$$

for arbitrary ψ. This leads to the formal decomposition of the adjoint operator given by

$$\widehat{L}^{\dagger}\psi = \widehat{L}_n^{\dagger}\psi - \sum_{j\neq n}\delta(U_j-\kappa)w*\psi+\mathcal{O}(\varepsilon) \tag{2.30}$$

for any $n=1,\ldots,N$, with $\delta(U_n-\kappa)$ satisfying (2.22). Without loss of generality, set $x_0=0$ and look for solutions of $\widehat{L}_0^{\dagger}\mathcal{P}=0$, which can be written as

$$\mathcal{P}(x) = \left[\frac{\delta(x+a)}{U'(-a)}+\frac{\delta(x-a)}{|U'(a)|}\right]\int_{-\infty}^{\infty} w(x-x')\mathcal{P}(x')dx'. \tag{2.31}$$

The formal solution is $\mathcal{P}(x)=p_1\delta(x-a)-p_2\delta(x+a)$, with coefficients p_1,p_2 satisfying the pair of algebraic equations

$$p_1 = \frac{1}{|U'(a)|}\left[p_1w(0)-p_2w(2a)\right],$$

$$p_2 = -\frac{1}{U'(-a)}\left[p_1w(2a)-p_2w(0)\right].$$

Differentiating (2.6) shows that

$$U'(-a) = -U'(a) = w(0)-w(2a), \tag{2.32}$$

and hence $p_1=p_2$. This establishes that $\widehat{L}_0^{\dagger}$ has the null vector

$$\mathcal{P}(x) = \delta(x-a)-\delta(x+a). \tag{2.33}$$

From translation symmetry, it follows that $\widehat{L}_n^{\dagger}$ has the null vector $P_n(x)$, where

$$P_n(x) \equiv \mathcal{P}(x-x_n). \tag{2.34}$$

Hence, using the decomposition (2.30) and the result $\widehat{L}_n^{\dagger}P_n=0$, we have

$$\langle \widehat{L}^{\dagger}P_n|Q\rangle = -\sum_{j\neq n}\langle\delta(U_j-\kappa)w*P_n|Q\rangle+\mathcal{O}(\varepsilon) \tag{2.35}$$

for any bounded function Q. Since $w(x)$ decays as $\mathrm{e}^{-\rho|x|}$ for large $|x|$, we see that $w(x_n-x_j)\sim\varepsilon^{|n-j|}$ for $n\neq j$, so that the inner product on the right-hand side of (2.35) is also $\mathcal{O}(\varepsilon)$. We conclude that (2.28) has the set of solutions P_n, $n=1,\ldots,N$. Interestingly, these solutions are independent of the choice of weight function w.

We now take the inner product of (2.19) with respect to P_m and use (2.23). Keeping only leading-order terms in ε then yields the following solvability condition:

$$\dot{\phi}_m\left\langle P_m\,|U_m'\right\rangle + \frac{1}{\varepsilon}\left\langle P_m\,|w*\delta(U_m-\kappa)[U_{m+1}+U_{m-1}]\right\rangle = \mathcal{O}(\varepsilon). \tag{2.36}$$

Substituting (2.33) into (2.36) and using (2.22), (2.32) shows that

$$\langle P_m\,|w*\delta(U_m-\kappa)[U_{m+1}+U_{m-1}]\rangle = U(a+x_m-x_{m+1})+U(a+x_m-x_{m-1}) - U(-a+x_m-x_{m+1})-U(-a+x_m-x_{m-1})$$

(2.37)

and

$$\langle P_m\,|U_m'\rangle = [U_m'(a+x_m)-U_m'(-a+x_m)] = -2|U'(a)|. \tag{2.38}$$

We thus obtain the following system of differential equations for the pulse positions $x_m(t) = md + \phi_m(\varepsilon t)$:

$$\begin{aligned} &\dot{x}_m = f(x_{m+1}-x_m) - f(x_m - x_{m-1}), \quad 1 < m < N, \\ &\dot{x}_1 = f(x_2-x_1), \quad \dot{x}_N = -f(x_N - x_{N-1}) \end{aligned} \tag{2.39}$$

with

$$f(x) = \frac{1}{2|U'(a)|}\left[U(x-a)-U(x+a)\right]. \tag{2.40}$$

2.3. Stationary *N*-pulses. Equations (2.6) and (2.40) show that the explicit form of the interaction function $f(x)$ for large x is determined by the asymptotic behavior of the weight distribution w. In the case of the Mexican hat function (2.8), equations (2.6), (2.9), and (2.40) imply that for large x

$$f(x) = -\frac{\Gamma\cosh(\sigma_I a)}{\sigma_I|U'(a)|}\left[\mathrm{e}^{-\sigma_I(x-a)} - \mathrm{e}^{-\sigma_I(x+a)}\right] = -Ae^{-\sigma_I x} \tag{2.41}$$

with

$$A = \frac{\Gamma\sinh(2\sigma_I a)}{\sigma_I|U'(a)|} > 0. \tag{2.42}$$

Similarly, in the case of a spatially decaying oscillatory function (2.11), we find that for large x,

$$f(x) = \frac{2\mathrm{e}^{-\sigma x}}{(1+\sigma^2)|U'(a)|}\left[A_1(a,\sigma)\cos(x) + A_2(a,\sigma)\sin(x)\right] \tag{2.43}$$

with

$$A_1(a,\sigma) = (1-\sigma^2)\sinh(\sigma a)\sin(a) + 2\sigma\cosh(\sigma a)\cos(a) - 2\sigma, \tag{2.44}$$

$$A_2(a,\sigma) = 2\sigma\sinh(\sigma a)\sin(a) - (1-\sigma^2)\cosh(\sigma a)\cos(a) + 1 - \sigma^2. \tag{2.45}$$

The function f can be written in the more compact form

$$f(x) = B\mathrm{e}^{-\sigma x}\cos(x-\Phi) \tag{2.46}$$

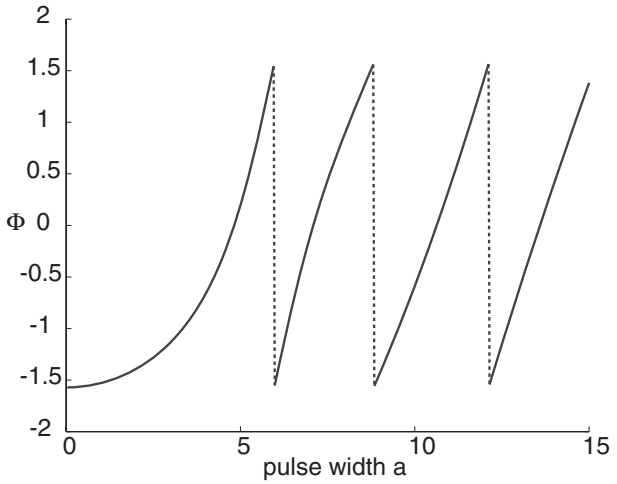

FIG. 2.4. *Plot of phase separation* Φ *for a pair of pulses as a function of pulse width* a *in the case of the spatially decaying oscillatory weight distribution* (2.11) *with* $\sigma = 0.25$.

with

$$\Phi = \tan^{-1}\frac{A_2}{A_1}, \quad B = \frac{2\sqrt{A_1^2 + A_2^2}}{(1+\sigma^2)|U'(a)|}. \tag{2.47}$$

The dependence of the phase Φ on pulse width for fixed decay rate σ is shown in Figure 2.4. Note that for $\sigma a \gg 1$ we have $\Phi \approx a - \phi$ with $\tan\phi = (1-\sigma^2)/2\sigma$.

The existence and stability of stationary N-pulse solutions can now be investigated in terms of the fixed point solutions of (2.39) for a given weight distribution. Let us first consider a pair of pulses, whose positions satisfy the pair of equations

$$\dot{x}_1 = f(x_2 - x_1), \quad \dot{x}_2 = -f(x_2 - x_1). \tag{2.48}$$

Defining the separation variable $\Delta = x_2 - x_1$, we have

$$\dot{\Delta} = -2f(\Delta). \tag{2.49}$$

It immediately follows from (2.41) that mutual interactions between pulses are repulsive for a Mexican hat weight function, since $f(\Delta) < 0$ for all Δ. Hence, the pulses repel each other and cannot form a bound 2-pulse state. A similar result holds for more than two pulses. Note that Amari [1] originally suggested that pulses were attractive at short distances, repulsive at intermediate distances, and neutral at sufficiently large distances. Our analysis suggests that repulsion actually persists to arbitrarily large distances, but that the rate of separation is slow since $f(\Delta) \sim \mathrm{e}^{-\sigma_I \Delta} \ll 1$. Following the results of Laing and colleagues [25, 27] and analogous results for PDEs [2], one expects a stable N-pulse solution to exist when the weights have an oscillatory tail. This is easily seen in the case for a pair of pulses by substituting (2.46) into (2.49):

$$\dot{\Delta} = -2B\mathrm{e}^{-\sigma\Delta}\cos(\Delta - \Phi). \tag{2.50}$$

Such an equation has a countable set of stable/unstable pairs of fixed point solutions: $\Delta = \Delta_\pm(p) = \Phi \pm \pi/2 + 2\pi p$ for integers $p \gg 1$ (so that pulses are well separated) with $\Delta_-(p)$ stable and $\Delta_+(p)$ unstable.

Higher-order N-pulse solutions can be constructed by taking the separations $\Delta_m = x_m - x_{m-1}$ to be zeros of f for all $m = 2, \ldots, N$. Stability is determined by the eigenvalues of the tridiagonal matrix

$$\mathbf{A}_N = \begin{pmatrix} -2f'(\Delta_2) & f'(\Delta_3) & 0 & \ldots & 0 \\ f'(\Delta_2) & -2f'(\Delta_3) & f'(\Delta_4) & 0 & \ldots \\ 0 & f'(\Delta_3) & -2f'(\Delta_4) & f'(\Delta_5) & 0 \\ \vdots & \vdots & \vdots & \vdots & \vdots \\ 0 & \ldots & 0 & f'(\Delta_{N-1}) & -2f'(\Delta_N) \end{pmatrix}. \tag{2.51}$$

Note that the matrix coefficients satisfy $a_{i,i+1} = a_{i+1,i} > 0$ for all i so that the eigenvalues are all real and simple. Moreover, by the Gerschgorin disk theorem (see [22]), the eigenvalues of $\mathbf{A}_N$ are contained in the union of disks defined according to $\cup_i \{|\lambda - a_{ii}| \leq \sum_{j \neq i} |a_{ij}|\}$. Consider the simplest case in which all pulse spacings are equal, $\Delta_m = \Delta$ for all $m = 2, \ldots, N$. We then obtain the pair of conditions

$$|\lambda + 2f'(\Delta)| \leq f'(\Delta), \quad |\lambda + 2f'(\Delta)| \leq 2f'(\Delta). \tag{2.52}$$

These are circles contained within the left-half complex plane, provided that $f'(\Delta) > 0$. One can also show that there are no zero eigenvalues by noting that in the uniform case the determinant $D_N = \det[\mathbf{A}_N - \lambda \mathbf{I}]$ satisfies the iterative equation

$$D_m(\lambda) = (-2f'(\Delta) - \lambda) D_{m-1} - f'(\Delta)^2 D_{m-2}, \quad 2 \leq m \leq N, \tag{2.53}$$

with $D_1 = 1$ and $D_0 = 0$. This has the solution

$$D_N(\lambda) = \frac{\Lambda_+^N - \Lambda_-^N}{\Lambda_+ - \Lambda_-}, \tag{2.54}$$

where

$$\Lambda_\pm = \frac{1}{2}\left(-2f' - \lambda \pm \sqrt{\lambda^2 + 4f'\lambda}\right). \tag{2.55}$$

Since $D_N(0) \neq 0$, it follows that zero is not an eigenvalue. Therefore, there exists a stable uniformly spaced stationary N-pulse solution if $f(\Delta) = 0$ and $f'(\Delta) > 0$.

One can also analyze the stationary states of N pulses arranged on a ring of length L. Now the dynamics is described by the cyclic system of ODEs

$$\dot{x}_m = f(x_{m+1} - x_m) - f(x_m - x_{m-1}), \quad m = 1, \ldots, N, \tag{2.56}$$

with $x_0 = x_N$ and $x_{N+1} = x_0$. The evenly spaced solution $\Delta = L/N$ is automatically a fixed point of the dynamics, and its stability can be determined by linearizing (2.56) with $x_m = m\Delta + \theta_m$:

$$\dot{\theta}_m = -f'(\Delta)\left[2\theta_m - \theta_{m-1} - \theta_{m+1}\right]. \tag{2.57}$$

This has eigensolutions of the form $\theta_m(t) = \mathrm{e}^{\lambda(k)t}\mathrm{e}^{imk}$ with wavenumber $k = 2\pi p/N$ for $p = 1, \ldots, N$ and

$$\lambda(k) = -2f'(\Delta)[1 - \cos(k)]. \tag{2.58}$$

The zero eigenvalue at $k = 0$ reflects the translation invariance of the system. Hence, the N-pulse solution on the ring is (marginally) stable if $f'(\Delta) > 0$; otherwise it is

unstable. It then follows from (2.41) and (2.46) that a ring network with a Mexican hat weight distribution supports stable N-pulse solutions independently of the length L of the ring, whereas a spatially decaying oscillatory distribution supports such a solution only for certain ranges of L. This example illustrates how the existence and stability of multipulse solutions depends on the topology of the network as well as its weight distribution.

3. Traveling pulses in asymmetric lateral inhibition networks. In section 2 we considered a lateral inhibition network with a weight distribution that is symmetric, $w(-x) = w(x)$. Although this is usually a reasonable modeling assumption regarding the large-scale anatomy of cortical circuits, there are some examples of more specialized circuits where lateral inhibition may be asymmetric. In particular, asymmetric coupling has been suggested as providing a possible mechanism for direction selective neurons in the visual cortex [38, 30, 32, 43]. Networks with asymmetric lateral inhibition support unidirectional wave propagation rather than stationary activity pulses. If a moving external stimulus is presented to a one-dimensional network, then a superthreshold response is elicited only if the velocity of the stimulus approximately matches the direction and speed of the intrinsic waves. Here we extend the singular perturbation theory of stationary pulses in order to investigate traveling N-pulse solutions of (2.1) in the case of asymmetric lateral inhibition.

3.1. Traveling solitary pulses. Suppose that (2.1) with asymmetric w has a right-moving traveling pulse solution of the form $u(x,t) = U(x-ct)$, $c > 0$, where $U(\pm\infty) = 0$ and $U(-a) = U(0) = \kappa$. Substituting into (2.1) with $\xi = x - ct$ gives

$$\begin{aligned} -c\partial_\xi U(\xi) + U(\xi) &= \int_{-\infty}^{\infty} w(\xi - \xi')H(U(\xi') - \kappa)d\xi' \\ &= W(\xi + a) - W(\xi), \end{aligned} \tag{3.1}$$

with W defined by (2.5). Multiplying both sides of (3.1) by the integrating factor $-c^{-1}\mathrm{e}^{-\xi/c}$ and integrating from $-a$ to ξ using the threshold condition $U(-a) = \kappa$ leads to the result

$$U(\xi) = \mathrm{e}^{\xi/c}\left[\kappa\mathrm{e}^{a/c} - \frac{1}{c}\int_{-a}^{\xi}[W(\xi' + a) - W(\xi')]\mathrm{e}^{-\xi'/c}d\xi'\right]. \tag{3.2}$$

Finiteness of the solution in the limit $\xi \to \infty$ requires that the term in square brackets vanish. Hence, we can rewrite the solution for $U(\xi)$ as

$$U(\xi) = \frac{1}{c}\int_0^{\infty}(W(\xi' + \xi + a) - W(\xi' + \xi))\mathrm{e}^{-\xi'/c}d\xi'. \tag{3.3}$$

Enforcing the threshold conditions $U(0) = \kappa$ and $U(-a) = \kappa$ then generates a pair of equations that determine existence curves relating the speed c to the pulse width a for a given threshold κ.

A typical way to model asymmetric lateral inhibition is to take $w(x) = w_0(x - x_0)$ with w_0 a symmetric weight distribution such as a Mexican hat function. If $x_0 > 0$, then short-range coupling is predominantly excitatory to the right and inhibitory to the left, which leads to right-propagating waves, as illustrated in Figure 3.1. The function $W(x)$ of (2.9) may be expressed in terms of w_0 as

$$W(x) = W_0(x - x_0) + W_0(x_0), \quad W_0(x) = \int_0^x w_0(y)dy, \tag{3.4}$$

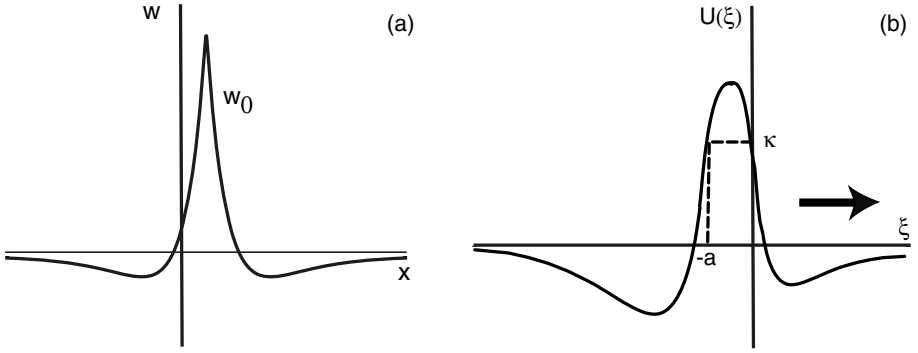

FIG. 3.1. (a) *Shifted weight distribution* $w(x) = w(x - x_0)$ *in the case of asymmetric lateral inhibition.* (b) *Illustration of a right-moving traveling pulse of width* a.

so that the wave profile becomes

$$U(\xi) = \frac{1}{c}\int_0^\infty (W_0(\xi' + \xi + a - x_0) - W_0(\xi' + \xi - x_0))\mathrm{e}^{-\xi'/c}d\xi'. \tag{3.5}$$

Equation (3.5) can be used to determine the asymptotic behavior of the solitary pulse for any exponentially decaying weight distribution. In particular, suppose that

$$w_0(x) = \mathrm{e}^{-\sigma|x|}g(x),$$

with $g(x)$ bounded for all x and $\lim_{x\to\pm\infty} g(x) = g_{\pm\infty}$. If $\xi > x_0$, then there is a common factor of $\mathrm{e}^{-\sigma\xi}$ on the right-hand side of (3.5), which can be taken outside the integral. Hence, in the limit $\xi \to \infty$,

$$U(\xi) \sim \frac{g_\infty}{c}\int_0^\infty (\mathrm{e}^{-\sigma(\xi'+\xi+a-x_0)} - \mathrm{e}^{-\sigma(\xi'+\xi-x_0)})\mathrm{e}^{-\xi'/c}d\xi' \sim -\mathrm{e}^{-\sigma\xi}. \tag{3.6}$$

On the other hand, when $\xi < x_0$, we have to partition the integral of (3.5) into the separate domains $\xi' > \xi + x_0$, $\xi + x_0 - a < \xi' < \xi + x_0$, and $\xi' < \xi + x_0 - a$ so that in the limit $\xi \to -\infty$,

$$U(\xi) \sim -\left[U_1\mathrm{e}^{\sigma\xi} + U_2\mathrm{e}^{\xi/c}\right]. \tag{3.7}$$

Therefore, the leading edge of the pulse profile decays at the rate σ determined by the weight distribution w_0, whereas the trailing edge decays at the rates σ and c^{-1}. The activity profile $U(\xi)$ of both the leading and trailing edges is negative due to the effects of inhibition; see Figure 3.1b. If $g(x)$ is taken to be an oscillatory function, then the asymptotic terms $\mathrm{e}^{-\sigma|\xi|}$ will also be oscillatory.

In Figure 3.2 we show existence curves for a traveling pulse of width a and speed c with w_0 given by the difference-of-exponentials (2.8). The pulse profile is given by $U(\xi) = U_{\sigma_E}(\xi) - \Gamma U_{\sigma_I}(\xi)$ with

$$\sigma U_\sigma(\xi) = \frac{\mathrm{e}^{-(\xi-x_0)\sigma}}{c\sigma+1} - \frac{\mathrm{e}^{-(\xi+a-x_0)\sigma}}{c\sigma+1}$$

for $\xi > x_0$,

$$\sigma U_\sigma(\xi) = 2 - \frac{\mathrm{e}^{-(\xi+a-x_0)\sigma}}{c\sigma+1} - \left[\left(\frac{2c^2\sigma^2}{c^2\sigma^2-1}\right)\mathrm{e}^{-(x_0-\xi)/c} - \frac{\mathrm{e}^{-(x_0-\xi)\sigma}}{c\sigma-1}\right]$$

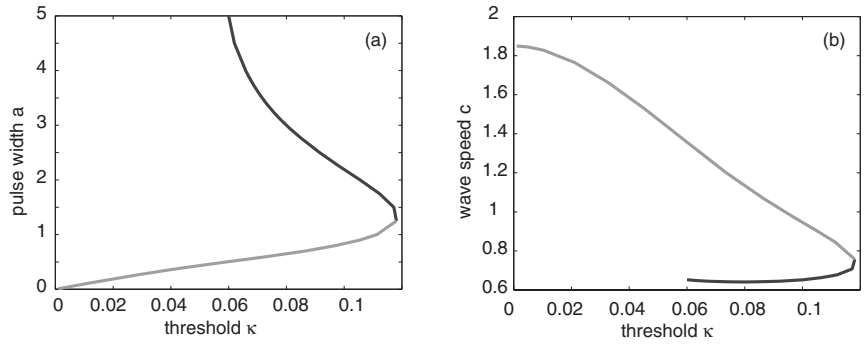

FIG. 3.2. *Existence of right-moving traveling pulses in the case of a shifted weight distribution* $w(x) = w_0(x - x_0)$ *with* $w_0(x)$ *given by the difference-of-exponentials* (2.8) *for* $\sigma_E = 1.8, \sigma_I = 1.0, \Gamma = 0.5$, *and* $x_0 = 0.5$. (a) *Plot of pulse width* a *against threshold* κ. (b) *Plot of wave speed* c *against threshold* κ. *Black (gray) curves denote stable (unstable) branches.*

for $x_0 - a < \xi < x_0$, and

$$\sigma U_\sigma(\xi) = \left[\left(\frac{2c^2\sigma^2}{c^2\sigma^2 - 1}\right) \mathrm{e}^{-(x_0-\xi-a)/c} - \frac{\mathrm{e}^{-(x_0-\xi-a)\sigma}}{c\sigma - 1}\right] - \left[\left(\frac{2c^2\sigma^2}{c^2\sigma^2 - 1}\right) \mathrm{e}^{-(x_0-\xi)/c} - \frac{\mathrm{e}^{-(x_0-\xi)\sigma}}{c\sigma - 1}\right]$$

for $\xi < x_0 - a$. Note that there are two existence branches corresponding, respectively, to narrow fast waves and wide slow waves. Given that wide pulses are stable in the stationary case (see Figure 2.1), we expect the slow branch to be stable, as can be confirmed numerically. This should be contrasted with traveling pulses in excitatory networks, where the fast branch is stable (see section 4). For the parameter values chosen in Figure 3.2, a stable pulse has a speed lying within the interval $0.6 < c < 0.8$ so that $\sigma_I < c^{-1} < \sigma_E$. Thus the dominant rate of decay for both the leading and trailing edges is σ_I. Note that if the units of length and time are taken to be 200μm and 10ms, respectively, then $c = 1$ corresponds to a wave speed of $2\mathrm{cms}^{-1}$, which is consistent with the range of speeds observed experimentally in cortical slices [20].

3.2. Singular perturbation theory. Suppose that there is a set of well separated exponentially decaying right-moving pulses. Following Elphick, Meron, and Spiegel [10], we now extend the singular perturbation theory of stationary pulses by working in the moving frame $\xi = x - ct$, where c is the speed of an isolated pulse. That is, we search for a traveling N-pulse solution with individual pulses having centers at $\xi_n = nd + \phi_n(\tau)$, where $\tau = \varepsilon t$ and $\varepsilon = \mathrm{e}^{-\rho d}$ with $\rho = \min\{\sigma, c^{-1}\}$:

$$u(\xi, \tau) = \sum_{n=1}^{N} U(\xi - nd - \phi_n(\tau)) + \varepsilon R(\xi, \tau). \tag{3.8}$$

Substituting (3.8) into (2.1) with $\partial_t \to \partial_t + \varepsilon\partial_\tau$, and performing an expansion in ε along lines identical to those of section 2, leads to the inhomogeneous equation (2.19), with the modified linear operator

$$\widehat{L}\psi = \psi - c\partial_\xi\psi - w * \left[\delta\left(\sum_{n=1}^{N} U_n - \kappa\right)\psi\right]. \tag{3.9}$$

The corresponding adjoint operator is now

$$\widehat{L}^{\dagger}\psi = \psi + c\partial_{\xi}\psi - \delta\left(\sum_{n=1}^{N} U_n - \kappa\right) w^T * \psi, \tag{3.10}$$

where $w^T(\xi) = w(-\xi) \neq w(\xi)$, since w is asymmetric. By differentiating (3.1), it can be seen that for largely separated pulses the functions U_n' are $\mathcal{O}(\varepsilon)$ null vectors of the operator $\widehat{L}$. This motivates us to seek $\mathcal{O}(\varepsilon)$ null vectors of the adjoint operator (3.10).

Proceeding along lines identical to those of section 2, we first decompose $\widehat{L}^{\dagger}$ according to (2.30) with

$$\widehat{L}_n^{\dagger}\psi = \psi + c\partial_{\xi}\psi - \delta(U_n - \kappa)w^T * \psi \tag{3.11}$$

and

$$\delta(U_n - \kappa) = \frac{\delta(\xi + a)}{U'(-a)} + \frac{\delta(\xi)}{|U'(0)|}. \tag{3.12}$$

We then look for null vectors $\mathcal{P}$ of $\widehat{L}_0^{\dagger}$ with $\xi_0 = 0$:

$$\mathcal{P}(\xi) + c\partial_{\xi}\mathcal{P}(\xi) = \left[\frac{\delta(\xi + a)}{U'(-a)} + \frac{\delta(\xi)}{|U'(0)|}\right] \int_{-\infty}^{\infty} w(\xi' - \xi)\mathcal{P}(\xi')d\xi'. \tag{3.13}$$

This has the formal solution

$$\mathcal{P}(\xi) = p_1 H(\xi + a)\mathrm{e}^{-(\xi+a)/c} - p_2 H(\xi)\mathrm{e}^{-\xi/c}, \tag{3.14}$$

with

$$p_1 c = \frac{1}{U'(-a)}\left[p_1 \int_0^{\infty} w(\xi)\mathrm{e}^{-\xi/c}d\xi - p_2 \int_0^{\infty} w(\xi + a)\mathrm{e}^{-\xi/c}d\xi\right]$$

and

$$p_2 c = -\frac{1}{|U'(0)|}\left[p_1 \int_0^{\infty} w(\xi - a)\mathrm{e}^{-\xi/c}d\xi - p_2 \int_0^{\infty} w(\xi)\mathrm{e}^{-\xi/c}d\xi\right].$$

Up to a scalar multiplication, the pair of algebraic equations for the coefficients p_1, p_2 has the solution

$$p_1 = \int_0^{\infty} w(\xi + a)\mathrm{e}^{-\xi/c}d\xi, \qquad p_2 = \int_0^{\infty} w(\xi - a)\mathrm{e}^{-\xi/c}d\xi. \tag{3.15}$$

In order to prove this, differentiate (3.3) with respect to ξ using (2.5):

$$U'(\xi) = \frac{1}{c}\int_0^{\infty} (w(\xi' + \xi + a) - w(\xi' + \xi))\mathrm{e}^{-\xi'/c}d\xi'. \tag{3.16}$$

Setting $\xi = 0$ and $\xi = -a$ then leads to the following equations for $U'(-a)$ and $|U'(0)|$:

$$\begin{aligned} U'(-a) &= \frac{1}{c}\int_0^{\infty} [w(\xi) - w(\xi - a)]\,\mathrm{e}^{-\xi/c}d\xi, \\ |U'(0)| &= \frac{1}{c}\int_0^{\infty} [w(\xi) - w(\xi + a)]\,\mathrm{e}^{-\xi/c}d\xi. \end{aligned} \tag{3.17}$$

It is now straightforward to verify (3.15).

Following the same arguments as section 2, we conclude that (2.28) has solutions of the form $P_n(\xi) = \mathcal{P}(\xi - \xi_n)$, with $\mathcal{P}$ given by (3.14) and (3.15). A dynamical equation for the pulse positions ξ_n can then be derived by taking the inner product of (2.19) with P_n, which yields an equation of the form (2.36). Substituting (3.14) and (3.12) into (2.36), we find that

$$\begin{aligned}\langle P_m \,|w * \delta(U_m - \kappa)[U_{m+1} + U_{m-1}]\rangle \\ = p_1 c\,(U(-a + \xi_m - \xi_{m+1}) + U(-a + \xi_m - \xi_{m-1})) \\ - p_2 c(U(\xi_m - \xi_{m+1}) + U(\xi_m - \xi_{m-1})),\end{aligned} \tag{3.18}$$

and $\langle P_m | U'_m \rangle = \langle \mathcal{P} | U' \rangle = K$, where

$$K = p_1 \int_0^\infty \mathrm{e}^{-\xi/c} U'(\xi - a) d\xi - p_2 \int_0^\infty \mathrm{e}^{-\xi/c} U'(\xi) d\xi. \tag{3.19}$$

Hence, (2.36) reduces to the form

$$\dot{\xi}_m = f_R(\xi_{m+1} - \xi_m) + f_L(\xi_m - \xi_{m-1}), \tag{3.20}$$

for $\xi_m(t) = nd + \phi_m(\varepsilon t)$, with

$$f_R(\xi) = \frac{c}{K}\left[p_2 U(-\xi) - p_1 U(-\xi - a)\right], \qquad f_L(\xi) = \frac{c}{K}\left[p_2 U(\xi) - p_1 U(\xi - a)\right], \tag{3.21}$$

and $U(\xi)$ determined from the underlying weight distribution according to (3.5).

3.3. Traveling wave trains. Lattice equations of the form (3.20) have been studied in considerable detail within the context of diffusive excitable systems and fluids [10, 2, 37]. Here we illustrate some of the basic results by explicitly calculating the interaction functions f_L, f_R. We define a traveling wave train as an N-pulse solution of (3.20) in which $\dot{\xi}_m = \delta c$ independently of m, where δc is a constant velocity in the frame of an isolated pulse. The spacings between pulses are then fixed, and we obtain the so-called pattern map [10]

$$\delta c = f_R(\Delta_{m+1}) + f_L(\Delta_m), \quad \Delta_m = \xi_m - \xi_{m-1}. \tag{3.22}$$

As a further simplification, we impose periodic boundary conditions by taking the pulses to be moving on a ring of length L with $\xi_0 = \xi_N$ and $\xi_{N+1} = \xi_0$. The simplest solution of (3.22) is then the fixed point $\Delta_m = \Delta = L/N$ for all m. The fixed point equation $\delta c = f_R(\Delta) + f_L(\Delta)$ determines the relationship between the total speed of the wave train $c + \delta c$ and the uniform spacing Δ between neighboring pulses. Linearizing (3.20) about the uniformly spaced wave train by setting $\xi_m = m\Delta + \delta c t + \theta_m$ gives

$$\dot{\theta}_m = f'_R(\Delta)\left[\alpha\theta_{m-1} - (1 + \alpha)\theta_m + \theta_{m+1}\right] \tag{3.23}$$

with $\alpha = -f'_L(\Delta)/f'_R(\Delta)$. This has eigensolutions of the form $\theta_m(t) = \mathrm{e}^{\lambda(k)t}\mathrm{e}^{imk}$

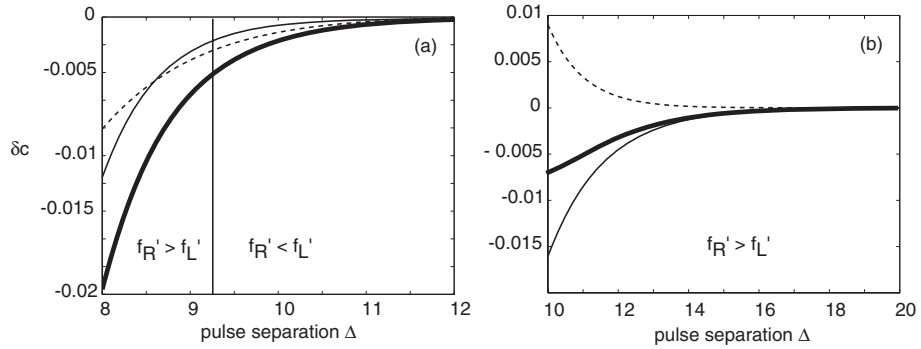

FIG. 3.3. *Plot of $\delta c = f_L(\Delta) + f_R(\Delta)$ against Δ (thick curves) in the case of a shifted weight distribution $w(x) = w_0(x - x_0)$, with $w_0(x)$ given by the difference-of-exponentials* (2.8) *for $\sigma_E = 1.8, \sigma_I = 1.0, \Gamma = 0.5$. Also shown are the plots of $f_L(\Delta)$ (dashed curves) and $f_R(\Delta)$ (thin curves).* (a) *$x_0 = 0.5$, $a = 5$, and $c = 0.65$.* (b) *$x_0 = 1$, $a = 4$, and $c = 1.58$. In both cases, the pulse width and speed of an isolated pulse are chosen to lie on the stable existence branch.*

with wavenumber $k = 2\pi p/N$ for $p = 1, \ldots, N$ and

$$\lambda(k) = -f_R'(\Delta)\left[(1+\alpha)(1-\cos(k)) \pm i(1-\alpha)\sin(k)\right]. \tag{3.24}$$

The condition for (marginal) stability of the uniformly spaced wave train is thus $f_R'(\Delta) > f_L'(\Delta)$. For the sake of illustration, consider the case of an asymmetric Mexican hat weight distribution $w(x) = w_0(x - x_0)$, with w_0 given by the difference-of-exponentials (2.8). Let the unperturbed pulse width a and speed c correspond to a solitary wave on the stable slow branch; see Figure 3.2. Two examples of dispersion curves δc versus Δ are shown in Figure 3.3. In (a), one sees that there exists a finite range of separations Δ for which $f_R'(\Delta) > f_L'(\Delta)$, corresponding to a finite band of stable wave trains. Similarly, (b) shows an example of a semi-infinite band of stable wave trains. In both examples, a given wave train moves more slowly than an isolated pulse, since $\delta c = f_L(\Delta) + f_R(\Delta) < 0$. Which wave train is actually selected will depend on initial conditions.

Suppose that we now allow for the possibility of an oscillatory weight distribution such as (2.11). If $\sigma_I < c^{-1}$, then the leading and trailing edges both consist of exponentially decaying spatial oscillations, so that for widely separated pulses the lattice dynamics takes the form

$$\begin{aligned}\dot{\xi}_m = {} & A_R \mathrm{e}^{-\sigma(\xi_{m+1}-\xi_m)} \cos(\omega(\xi_{m+1}-\xi_m) - \Phi_R) \\ & + A_L \mathrm{e}^{-\sigma(\xi_m - \xi_{m-1})} \cos(\omega(\xi_m - \xi_{m-1}) - \Phi_L).\end{aligned} \tag{3.25}$$

In the case of oscillatory interaction functions, the associated pattern map (3.22) can generate nontrivial sequences of pulse intervals $\{\ldots \Delta_{m-1}, \Delta_m, \Delta_{m+1}, \ldots\}$, including possibly chaotic sequences [17]. From a dynamical systems perspective, such wave trains can be reinterpreted in terms of nearly homoclinic orbits [2].

4. Traveling pulses in excitatory networks with adaptation. As our final example, let us return to the case of a symmetric weight distribution w, but now take w to be purely excitatory, as in the case of a disinhibited cortical slice [34]. In the absence of lateral inhibition, the scalar equation (2.1) no longer supports localized persistent states of activity but does exhibit traveling front solutions. In order to

obtain traveling localized pulses, it is necessary to introduce some form of adaptation. Therefore, following Pinto and Ermentrout [34], we extend the basic Amari model by considering the following system of equations:

$$\begin{aligned} \frac{\partial u(x,t)}{\partial t} &= -u(x,t) + \int_{-\infty}^{\infty} w(x-x')H(u(x',t)-\kappa)dx' - \beta v(x,t), \\ \frac{\partial v(x,t)}{\partial t} &= \gamma[-v(x,t)+u(x,t)], \end{aligned} \tag{4.1}$$

where $v(x,t)$ represents some form of negative feedback mechanism such as spike frequency adaptation or synaptic depression, with β, γ determining the relative strength and rate of feedback. We will extend the singular perturbation theory of section 3 in order to investigate traveling N-pulse solutions of (4.1) in the case of a positive exponentially decaying weight distribution w.

4.1. Traveling solitary pulses. In contrast to the asymmetric lateral inhibition network of section 3, the excitatory network given by (4.1) supports bidirectional wave propagation. Without loss of generality, let us consider a right-moving traveling pulse solution of the form $(u(x,t), v(x,t)) = (U(x-ct), V(x-ct))$ with $U(\pm\infty), V(\pm\infty) = 0$ and $U(-a) = U(0) = \kappa$. Substituting into (4.1) with $\xi = x - ct$ gives

$$\begin{aligned} -c\partial_\xi U(\xi) + U(\xi) + \beta V(\xi) &= \int_{-\infty}^{\infty} w(\xi-\xi')H(U(\xi')-\kappa)d\xi', \\ -c\partial_\xi V(\xi) + \gamma[V(\xi)-U(\xi)] &= 0. \end{aligned} \tag{4.2}$$

It is useful to rewrite (4.2) in the matrix form

$$\begin{pmatrix} 1 & \beta \\ -\gamma & \gamma \end{pmatrix} \begin{pmatrix} U \\ V \end{pmatrix} - c\partial_\xi \begin{pmatrix} U \\ V \end{pmatrix} = [W(\xi+a) - W(\xi)] \begin{pmatrix} 1 \\ 0 \end{pmatrix}. \tag{4.3}$$

We proceed by diagonalizing the left-hand side of (4.3) using the right eigenvectors $\mathbf{v}$ of the matrix

$$\mathbf{M} = \begin{pmatrix} 1 & \beta \\ -\gamma & \gamma \end{pmatrix}. \tag{4.4}$$

These are given by

$$\mathbf{v}_\pm = \begin{pmatrix} \gamma - \lambda_\pm \\ \gamma \end{pmatrix}, \tag{4.5}$$

with corresponding eigenvalues

$$\lambda_\pm = \frac{1}{2}\left[1 + \gamma \pm \sqrt{(1+\gamma)^2 - 4\gamma(1+\beta)}\right]. \tag{4.6}$$

Note that $\mathbf{v}_\pm e^{\lambda_\pm \xi/c}$ are the corresponding null vectors of the linear operator on the left-hand side of (4.3); that is, they generate the complementary solution. Performing the transformation

$$\begin{pmatrix} \widetilde{U} \\ \widetilde{V} \end{pmatrix} = \mathbf{T}^{-1} \begin{pmatrix} U \\ V \end{pmatrix}, \quad \mathbf{T} = \begin{pmatrix} \mathbf{v}_+ & \mathbf{v}_- \end{pmatrix}, \tag{4.7}$$

then gives the pair of equations

$$-c\partial_\xi \widetilde{U} + \lambda_+ \widetilde{U} = \eta_+[W(\xi+a) - W(\xi)],$$
$$-c\partial_\xi \widetilde{V} + \lambda_- \widetilde{V} = \eta_-[W(\xi+a) - W(\xi)], \tag{4.8}$$

with $\eta_\pm = \mp 1/(\lambda_+ - \lambda_-)$. Integrating the equation for $\widetilde{U}$ from $-a$ to ∞, we have

$$\widetilde{U}(\xi) = \mathrm{e}^{\lambda_+\xi/c}\left[\widetilde{U}(-a)\mathrm{e}^{a\lambda_+/c} - \frac{\eta_+}{c}\int_{-a}^{\xi} \mathrm{e}^{-\lambda_+\xi'/c}[W(\xi'+a) - W(\xi')]d\xi'\right]. \tag{4.9}$$

Finiteness of $\widetilde{U}$ in the limit $\xi \to \infty$ requires that the term in square brackets cancel. Hence, we can eliminate $\widetilde{U}(-a)$ to obtain the result

$$\widetilde{U}(\xi) = \frac{\eta_+}{c}\int_0^\infty \mathrm{e}^{-\lambda_+\xi'/c}[W(\xi'+\xi+a) - W(\xi'+\xi)]d\xi'. \tag{4.10}$$

Similarly,

$$\widetilde{V}(\xi) = \frac{\eta_-}{c}\int_0^\infty \mathrm{e}^{-\lambda_-\xi'/c}[W(\xi'+\xi+a) - W(\xi'+\xi)]d\xi'. \tag{4.11}$$

Performing the inverse transformation $U = (\gamma - \lambda_+)\widetilde{U} + (\gamma - \lambda_-)\widetilde{V}$, we have

$$U(\xi) = \frac{1}{c}\int_0^\infty \left[\chi_+\mathrm{e}^{-\lambda_+\xi'/c} + \chi_-\mathrm{e}^{-\lambda_-\xi'/c}\right][W(\xi'+\xi+a) - W(\xi'+\xi)]d\xi', \tag{4.12}$$

with $\chi_\pm = (\gamma - \lambda_\pm)\eta_\pm$. Using $\lambda_+ + \lambda_- = 1 + \gamma$, we can rewrite $\chi_\pm$ as

$$\chi_+ = \frac{1-\lambda_-}{\lambda_+ - \lambda_-}, \qquad \chi_- = \frac{\lambda_+ - 1}{\lambda_+ - \lambda_-}. \tag{4.13}$$

The threshold conditions $U(-a) = \kappa$ and $U(0) = \kappa$ then yield a pair of equations whose solutions determine existence curves relating the speed c and width a of a pulse to the threshold κ [34].

For the sake of illustration, let w be given by the exponential function (2.8) with $\Gamma = 0$ and $\sigma_E = \sigma$; that is, $w(x) = \mathrm{e}^{-\sigma|x|}$. In the domain $\xi > 0$, there is a common factor of $\mathrm{e}^{-\sigma\xi}$ in the integrand of (4.12) so that $U(\xi) = \kappa\mathrm{e}^{-\sigma\xi}$ for $\xi > 0$, provided that

$$\kappa = \frac{(c\sigma + \gamma)(1 - \mathrm{e}^{-a\sigma})}{c^2\sigma^2 + c\sigma(1+\gamma) + \gamma(1+\beta)}. \tag{4.14}$$

On the other hand, when $\xi < 0$, one has to partition the integral of (4.12) into the separate domains $\xi' > |\xi|$, $|\xi| - a < \xi' < |\xi|$, and $\xi' < |\xi| - a$. This then determines the second threshold condition as well as the asymptotic behavior of $U(\xi)$ in the limit $\xi \to -\infty$:

$$U(\xi) = U_+\mathrm{e}^{\lambda_+\xi/c} + U_-\mathrm{e}^{\lambda_-\xi/c} + U_0\mathrm{e}^{\sigma\xi}, \tag{4.15}$$

where the amplitudes $U_\pm$ and U_0 can be determined from matching conditions at the threshold crossing points [34, 15]. Note that the leading edge of the pulse is positive, whereas the trailing edge is negative due to the effects of adaptation. One finds that for sufficiently slow negative feedback (small γ) and large β there exist two pulse solutions, one narrow and slow and the other wide and fast. This is illustrated in Figure 4.1. Numerically, the fast solution is found to be stable [34]. Its stability can also be established analytically using Evans function techniques [44, 8, 16].

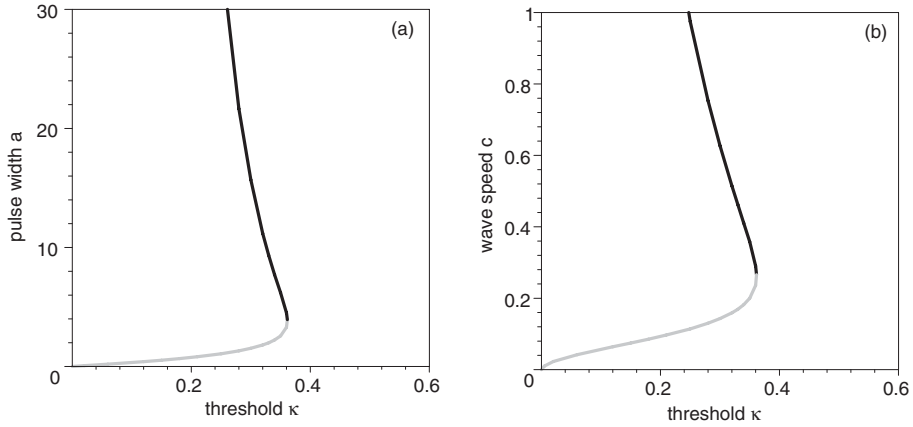

FIG. 4.1. *Existence of right-moving traveling pulses in the case of the excitatory network* (4.1) *for an exponential weight distribution with* $w(x) = e^{-\sigma|x|}$. *Here* $\sigma = 1, \gamma = 0.01$, *and* $\beta = 2.5$. (a) *Plot of pulse width* a *against threshold* κ. (b) *Plot of wave speed* c *against threshold* κ. *Stable (unstable) branches indicated by black (gray) curves.*

4.2. Singular perturbation theory. Suppose that (4.1) has a stable right-moving pulse solution $U(\xi)$ of width a and speed c. Following the model set by section 3, we search for a traveling N-pulse solution with individual pulses having centers at $\xi_n = nd + \phi_n(\tau)$, where $\tau = \varepsilon t$ and $\varepsilon = \mathrm{e}^{-\rho d}$ with $\rho = \min\{c^{-1}\lambda_{\pm}, \sigma\}$:

$$
\begin{aligned}
u(\xi,\tau) &= \sum_{n=1}^{N} U(\xi - nd - \phi_n(\tau)) + \varepsilon R(\xi,\tau),\\
v(\xi,\tau) &= \sum_{n=1}^{N} V(\xi - nd - \phi_n(\tau)) + \varepsilon \overline{R}(\xi,\tau).
\end{aligned}
\tag{4.16}
$$

Substituting (4.16) into (4.1) with $\partial_t \to \partial_t + \varepsilon\partial_\tau$, and using (4.2), gives

$$
\begin{aligned}
&-c\varepsilon\partial_\xi R + \varepsilon^2\partial_\tau R - \varepsilon\sum_{n=1}^{N}\dot{\phi}_n U_n'\\
&\qquad = -\varepsilon(R + \beta\overline{R}) + w * H\left(\sum_{n=1}^{N} U_n + \varepsilon R - \kappa\right) - w * \sum_{n=1}^{N} H(U_n - \kappa),\\
&-c\varepsilon\partial_\xi \overline{R} + \varepsilon^2\partial_\tau \overline{R} - \varepsilon\sum_{n=1}^{N}\dot{\phi}_n V_n' = -\varepsilon\gamma(\overline{R} - R).
\end{aligned}
\tag{4.17}
$$

Performing an expansion to $\mathcal{O}(\varepsilon)$ along lines identical to section 2 leads to the inhomogeneous equation

$$
\widehat{L}\begin{pmatrix} R \\ \overline{R} \end{pmatrix} = \sum_{n=1}^{N}\dot{\phi}_n\begin{pmatrix} U_n' \\ V_n' \end{pmatrix} + \frac{1}{\varepsilon} w * \left[H\left(\sum_{n=1}^{N} U_n - \kappa\right) - \sum_{n=1}^{N} H(U_n - \kappa)\right]\begin{pmatrix} 1 \\ 0 \end{pmatrix},
\tag{4.18}
$$

with the linear operator $\widehat{L}$ given by

$$\widehat{L}\psi = \begin{pmatrix} 1 & \beta \\ -\gamma & \gamma \end{pmatrix} \psi - c\partial_\xi \psi - w * \left[\delta \left(\sum_{n=1}^{N} U_n - \kappa \right) \begin{pmatrix} 1 & 0 \\ 0 & 0 \end{pmatrix} \psi \right], \tag{4.19}$$

where ψ now denotes a two-vector rather than a scalar. Differentiating (4.2) and using arguments similar to those of section 2, it is straightforward to show that $\widehat{L}(U_n', V_n')^{tr} = \mathcal{O}(\varepsilon)$ for all $n = 1, \ldots, N$. This again motivates us to seek $\mathcal{O}(\varepsilon)$ null vectors of the adjoint operator.

In order to determine the corresponding solvability conditions on (4.18), we seek weak solutions $(P, \overline{P})$ of the equation

$$\left\langle \widehat{L}^\dagger \begin{pmatrix} P \\ \overline{P} \end{pmatrix} \middle| \begin{pmatrix} Q \\ \overline{Q} \end{pmatrix} \right\rangle = \mathcal{O}(\varepsilon) \tag{4.20}$$

for arbitrary bounded functions $Q, \overline{Q}$, where $\widehat{L}^\dagger$ is the adjoint operator

$$\widehat{L}^\dagger \psi = \begin{pmatrix} 1 & -\gamma \\ \beta & \gamma \end{pmatrix} \psi + c\partial_\xi \psi - \delta \left(\sum_{n=1}^{N} U_n - \kappa \right) w * \left[\begin{pmatrix} 1 & 0 \\ 0 & 0 \end{pmatrix} \psi \right]. \tag{4.21}$$

The inner product is defined by first taking the dot product of the two vectors and then integrating over $\mathbf{R}$. Using the perturbation expansion (2.29) with $\delta(U_n - \kappa)$ given by (3.12), we obtain the following formal decomposition:

$$\widehat{L}^\dagger \psi = \widehat{L}_n^\dagger \psi - \sum_{j \neq n} \delta(U_j - \kappa) w * \left[\begin{pmatrix} 1 & 0 \\ 0 & 0 \end{pmatrix} \psi \right] + \mathcal{O}(\varepsilon) \tag{4.22}$$

for any $n = 1, \ldots, N$, with

$$\widehat{L}_n^\dagger \psi = \begin{pmatrix} 1 & -\gamma \\ \beta & \gamma \end{pmatrix} \psi + c\partial_\xi \psi - \delta(U_n - \kappa) w * \left[\begin{pmatrix} 1 & 0 \\ 0 & 0 \end{pmatrix} \psi \right]. \tag{4.23}$$

We now look for null vectors of $\widehat{L}_0^\dagger$ with $\xi_0 = 0$. We proceed by partially diagonalizing $\widehat{L}_0^\dagger$ using the left eigenvectors $\widetilde{\mathbf{v}}$ of the matrix $\mathbf{M}$ (see (4.4)):

$$\widetilde{\mathbf{v}}_\pm = \begin{pmatrix} \gamma \\ 1 - \lambda_\pm \end{pmatrix}. \tag{4.24}$$

Introducing the transformation

$$\begin{pmatrix} \mathcal{Q} \\ \overline{\mathcal{Q}} \end{pmatrix} = \widetilde{\mathbf{T}}^{-1} \begin{pmatrix} \mathcal{P} \\ \overline{\mathcal{P}} \end{pmatrix}, \quad \widetilde{\mathbf{T}} = \begin{pmatrix} \widetilde{\mathbf{v}}_+ & \widetilde{\mathbf{v}}_- \end{pmatrix}, \tag{4.25}$$

then leads to the following pair of equations:

$$c\partial_\xi \mathcal{Q} + \lambda_+ \mathcal{Q} = \chi_+ \delta(U - \kappa) w * [\mathcal{Q} + \overline{\mathcal{Q}}], \tag{4.26}$$

$$c\partial_\xi \overline{\mathcal{Q}} + \lambda_- \overline{\mathcal{Q}} = \chi_- \delta(U - \kappa) w * [\mathcal{Q} + \overline{\mathcal{Q}}], \tag{4.27}$$

with $\chi_\pm$ defined by (4.13). Using an analysis similar to that of section 3, we obtain the solution

$$\begin{aligned} \mathcal{Q}(\xi) &= \chi_+ \left[p_1 H(\xi + a) \mathrm{e}^{-\lambda_+(\xi+a)/c} - p_2 H(\xi) \mathrm{e}^{-\lambda_+ \xi/c} \right], \\ \overline{\mathcal{Q}}(\xi) &= \chi_- \left[p_1 H(\xi + a) \mathrm{e}^{-\lambda_-(\xi+a)/c} - p_2 H(\xi) \mathrm{e}^{-\lambda_- \xi/c} \right], \end{aligned} \tag{4.28}$$

with p_1, p_2 given by (3.15) and $U'(0), U'(-a)$ satisfying the self-consistency conditions

$$c = \frac{1}{U'(-a)} \int_0^\infty [w(\xi) - w(\xi - a)] \left[\chi_+ \mathrm{e}^{-\lambda_+ \xi/c} + \chi_- \mathrm{e}^{-\lambda_- \xi/c}\right] d\xi,$$

$$c = \frac{1}{U'(0)} \int_0^\infty [w(\xi + a) - w(\xi)] \left[\chi_+ \mathrm{e}^{-\lambda_+ \xi/c} + \chi_- \mathrm{e}^{-\lambda_- \xi/c}\right] d\xi. \tag{4.29}$$

The latter follow immediately from differentiating (4.12) and setting $\xi = 0, -a$. Finally, we perform the inverse transformation on $\mathcal{Q}, \overline{\mathcal{Q}}$ to obtain $\mathcal{P}, \overline{\mathcal{P}}$:

$$\begin{pmatrix} \mathcal{P}(\xi) \\ \overline{\mathcal{P}}(\xi) \end{pmatrix} = \chi_+ \begin{pmatrix} \gamma \\ 1 - \lambda_+ \end{pmatrix} \left[p_1 H(\xi + a) \mathrm{e}^{-\lambda_+(\xi+a)/c} - p_2 H(\xi) \mathrm{e}^{-\lambda_+ \xi/c}\right] + \chi_- \begin{pmatrix} \gamma \\ 1 - \lambda_- \end{pmatrix} \left[p_1 H(\xi + a) \mathrm{e}^{-\lambda_-(\xi+a)/c} - p_2 H(\xi) \mathrm{e}^{-\lambda_- \xi/c}\right]. \tag{4.30}$$

From translation symmetry, it follows that $\widehat{L}_n^\dagger$ has the null vector $(P_n, \overline{P}_n)$ with

$$P_n(\xi) = \mathcal{P}(\xi - \xi_n), \quad \overline{P}_n(\xi) = \overline{\mathcal{P}}(\xi - \xi_n). \tag{4.31}$$

Hence, applying the decomposition (4.22), we see that

$$\left\langle \widehat{L}^\dagger \begin{pmatrix} P_n \\ \overline{P}_n \end{pmatrix} \middle| \begin{pmatrix} Q \\ \overline{Q} \end{pmatrix} \right\rangle = -\sum_{j \neq n} \langle \delta(U_j - \kappa) w * P_n | Q \rangle + \mathcal{O}(\varepsilon). \tag{4.32}$$

Equations (4.30) and (4.31) imply that $P_n, \overline{P}_n$ are zero for $\xi < \xi_n - a$ and exponentially decaying for $\xi > \xi_n - a$. Evaluating the inner product on the right-hand side of (4.32) establishes that it is also $\mathcal{O}(\varepsilon)$. We conclude that (4.20) has the set of solutions $(P_n, \overline{P}_n)$, $n = 1, \ldots, N$. We now take the inner product of (4.18) with respect to the vector $(P_m, \overline{P}_m)$ for some integer $m, m = 1, \ldots, N$, and use (2.23):

$$\dot{\phi}_m \left\langle \begin{pmatrix} P_m \\ \overline{P}_m \end{pmatrix} \middle| \begin{pmatrix} U_m' \\ V_m' \end{pmatrix} \right\rangle + \frac{1}{\varepsilon} \langle P_m | w * \delta(U_m - \kappa)[U_{m+1} + U_{m-1}] \rangle = \mathcal{O}(\varepsilon). \tag{4.33}$$

Evaluating the various inner products using (4.30) and (3.12) leads to the same (3.20) and (3.21) as the scalar case, with

$$K = \gamma^{-1} \left\langle \begin{pmatrix} \mathcal{P} \\ \overline{\mathcal{P}} \end{pmatrix} \middle| \begin{pmatrix} U' \\ V' \end{pmatrix} \right\rangle. \tag{4.34}$$

However, there is a significant difference in the asymptotic behavior of the interaction functions f_L, f_R when compared to the scalar case. This is due to the fact that adaptation is slow ($\gamma \ll 1$) so that $\lambda_- \approx 0$, and thus the leading edge decays much faster than the trailing edge; see (4.6) and (4.15). Hence, we can neglect the interaction term f_L in (3.20) to obtain

$$\dot{\xi}_m = f_R(\xi_{m+1} - \xi_m) \tag{4.35}$$

with $f_R(\Delta) \sim -\mathrm{e}^{-\lambda_- \Delta/c}$. In this case the dynamics of the pulse position ξ_m depends only on the distance to the proceeding pulse $\Delta_m = \xi_{m+1} - \xi_m$ and can thus be reformulated within a kinematic framework [11, 33]. This is based on the observation that the function f_R directly determines the dispersion relation between the speed C and the pulse separation Δ of a uniformly spaced wave train, $C(\Delta) = f_R(\Delta) + c$. Thus

$$\dot{\xi_m} = C(\Delta_m) - c. \tag{4.36}$$

The condition for stability of a uniform wave train on a ring is then $f_R'(\Delta) > 0$.

5. Discussion. In this paper we have used perturbation methods to develop a theory of weakly interacting pulses in one-dimensional neuronal networks. We have shown how the pulse interactions explicitly depend on the form of the long-range synaptic coupling, and investigated how this determines the existence and stability of multipulse solutions. For simplicity, we have assumed throughout that the network is homogeneous: the coupling depends only on the distance between interacting elements in the network, and external inputs have been ignored. In a recent series of papers, we have shown that introducing a localized inhomogeneous input can generate oscillatory coherent states in the form of standing and traveling breathing pulses [5, 15, 16]. It would be interesting to develop a theory of weakly interacting breathers and to determine under what conditions long-range synaptic coupling can provide a mechanism for synchronizing the oscillations between breathers. This would provide an alternative way of thinking about stimulus-induced coherent oscillations in cortex, which are observed *in vivo* during periods of sensory processing [21, 14].

REFERENCES

[1] S. Amari, *Dynamics of pattern formation in lateral inhibition type neural fields*, Biol. Cybernet., 27 (1977), pp. 77–87.

[2] N. J. Balmforth, *Solitary waves and homoclinic orbits*, Ann. Rev. Fluid Mech., 27 (1995), pp. 335–373.

[3] N. J. Balmforth, G. R. Ierley, and R. Worthing, *Pulse dynamics in an unstable medium*, SIAM J. Appl. Math., 57 (1997), pp. 205–251.

[4] P. C. Bressloff, *Traveling waves and pulses in a one-dimensional network of excitable integrate-and-fire neurons*, J. Math. Biol., 40 (2000), pp. 169–198.

[5] P. C. Bressloff, S. Folias, A. Pratt, and Y.-X. Li, *Oscillatory waves in inhomogeneous neural media*, Phys. Rev. Lett., 91 (2003), paper 178101.

[6] R. D. Chervin, P. A. Pierce, and B. W. Connors, *Periodicity and directionality in the propagation of epileptiform discharges across neocortex*, J. Neurophysiol., 60 (1988), pp. 1695–1713.

[7] S. Coombes, G. J. Lord, and M. R. Owen, *Waves and bumps in neuronal networks with axo-dendritic synaptic interactions*, Phys. D, 178 (2003), pp. 219–241.

[8] S. Coombes and M. R. Owen, *Evans functions for integral neural field equations with Heaviside firing rate function*, SIAM J. Appl. Dyn. Syst., 3 (2004), pp. 574–600.

[9] C. Elphick, E. Meron, and E. A. Spiegel, *Spatiotemporal complexity in traveling patterns*, Phys. Rev. Lett., 61 (1988), pp. 496–499.

[10] C. Elphick, E. Meron, and E. A. Spiegel, *Patterns of propagating pulses*, SIAM J. Appl. Math., 50 (1990), pp. 490–503.

[11] C. Elphick, E. Meron, J. Rinzel and E. A. Spiegel, *Impulse patterning and relaxational propagation in excitable media*, J. Theoret. Biol., 146 (1990), pp. 249–268.

[12] G. B. Ermentrout, *Neural networks as spatial pattern forming systems*, Rep. Progr. Phys., 61 (1998), pp. 353–430.

[13] G. B. Ermentrout, *The analysis of synaptically generated traveling waves*, J. Comp. Neurosci., 5 (1998), pp. 191–208.

[14] G. B. Ermentrout and D. Kleinfeld, *Traveling electrical waves in cortex: Insights from phase dynamics and speculation on a computational role*, Neuron, 29 (2001), pp. 33–44.

[15] S. E. Folias and P. C. Bressloff, *Breathing pulses in an excitatory neural network*, SIAM J. Appl. Dyn. Syst., 3 (2004), pp. 378–407.

[16] S. E. Folias and P. C. Bressloff, *Stimulus-locked traveling pulses and breathers in an excitatory neural network*, SIAM J. Appl. Math., 65 (2005), pp. 2067–2092.

[17] A. C. Fowler and C. T. Sparrow, *Bifocal homoclinic orbits in four dimensions*, Nonlinearity, 4 (1991), pp. 1159–1182.

[18] J. M. Fuster and G. Alexander, *Neuron activity related to short-term memory*, Science, 173 (1971), pp. 652–654.

[19] C. D. Gilbert and T. N. Wiesel, *Clustered intrinsic connections in cat visual cortex*, J. Neurosci., 3 (1983), pp. 1116–1133.

[20] D. Golomb and Y. Amitai, *Propagating neuronal discharges in neocortical slices: Computational and experimental study*, J. Neurophysiol., 78 (1997), pp. 1199–1211.

[21] C. M. Gray, *Synchronous oscillations in neuronal systems: Mechanisms and functions*, J. Comput. Neurosci., 1 (1994), pp. 11–38.
[22] R. A. Horn and C. R. Johnson, *Matrix Analysis*, Cambridge University Press, Cambridge, UK, 1985.
[23] J. P. Keener, *Waves in excitable media*, SIAM J. Appl. Math., 39 (1980), pp. 528–548.
[24] C. R. Laing and C. C. Chow, *Stationary bumps in networks of spiking neurons*, Neural Comp., 13 (2001), pp. 1473–1494.
[25] C. R. Laing, W. C. Troy, B. Gutkin, and G. B. Ermentrout, *Multiple bumps in a neuronal model of working memory*, SIAM J. Appl. Math, 63 (2002), pp. 62–97.
[26] C. R. Laing and W. C. Troy, *Two-bump solutions of Amari-type models of neuronal pattern formation*, Phys. D, 178 (2003), pp. 190–218.
[27] C. R. Laing and W. C. Troy, *PDE methods for nonlocal models*, SIAM J. Appl. Dynam. Syst., 2 (2003), pp. 487–516.
[28] J. B. Levitt, D. A. Lewis, T. Yoshioka, and J. S. Lund, *Topography of pyramidal neuron intrinsic connections in macaque prefrontal cortex*, J. Comput. Neurol., 338 (1993), pp. 360–376.
[29] J. S. Lund, A. Angelucci, and P. C. Bressloff, *Anatomical substrates for functional columns in macaque monkey primary visual cortex*, Cerebral Cortex, 12 (2003), pp. 15–24.
[30] R. Maex and G. A. Orban, *Model circuit of spiking neurons generating directional selectivity in simple cells*, J. Neurophysiol., 75 (1996), pp. 1515–1545.
[31] B. A. McGuire, C. D. Gilbert, P. K. Rivlin, and T. N. Wiesel, *Targets of horizontal connections in macaque primary visual cortex*, J. Comput. Neurol., 305 (1991), pp. 370–392.
[32] P. Mineiro and D. Zipser, *Analysis of direction selectivity arising from recurrent cortical interactions*, Neural Comput., 10 (1998), pp. 353–371.
[33] M. Or-Guil, I. G. Kevrekidis, and M. Bar, *Stable bound states of pulses in an excitable medium*, Phys. D, 135 (2000), pp. 154–174.
[34] D. J. Pinto and G. B. Ermentrout, *Spatially structured activity in synaptically coupled neuronal networks*: I. *Traveling fronts and pulses*, SIAM J. Appl. Math., 62 (2001), pp. 206–225.
[35] D. J. Pinto and G. B. Ermentrout, *Spatially structured activity in synaptically coupled neuronal networks*: II. *Lateral inhibition and standing pulses*, SIAM J. Appl. Math., 62 (2001), pp. 226–243.
[36] K. S. Rockland and J. S. Lund, *Intrinsic laminar lattice connections in primate visual cortex*, J. Comput. Neurol., 216 (1983), pp. 303–318.
[37] C. P. Schenk, P. Schutz, M. Bode, and H. G. Purwins, *Interaction of self-organized quasi-particles in a two-dimensional reaction-diffusion system, The formation of molecules*, Phys. Rev. E, 57 (1998), pp. 6480–6486.
[38] H. Suarez, C. Koch, and R. Douglas, *Modeling direction selectivity of simple cells in striate visual cortex within the framework of the canonical microcircuit*, J. Neurosci., 15 (1995), pp. 6700–6719.
[39] X.-J. Wang, *Synaptic reverberation underlying mnemonic persistent activity*, Trends Neurosci., 24 (2001), pp. 455–463.
[40] H. Werner and T. Richter, *Circular stationary solutions in two-dimensional neural fields*, Biol. Cybernet., 85 (2001), pp. 211–217.
[41] H. R. Wilson and J. D. Cowan, *A mathematical theory of the functional dynamics of cortical and thalamic nervous tissue*, Kybernetik, 13 (1973), pp. 55–80.
[42] J-Y. Wu, L. Guan, and Y. Tsau, *Propagating activation during oscillations and evoked responses in neocortical slices*, J. Neurosci., 19 (1999), pp. 5005–5015.
[43] X. Xie and M. A. Giese, *Nonlinear dynamics of direction-selective recurrent neural media*, Phys. Rev. E, 65 (2002), paper 051904.
[44] L. Zhang, *On the stability of traveling wave solutions in synaptically coupled neuronal networks*, Differential Integral Equations, 16 (2003), pp. 513–536.